SUPPLEMENTAL MATERIAL

Mitochondria-Rich Extracellular Vesicles From Autologous Stem Cell-Derived Cardiomyocytes Restore Energetics of Ischemic Myocardium

Gentaro Ikeda, M.D., Ph.D.; Michelle R. Santoso, B.S.; Yuko Tada, M.D., Ph.D.; Albert M. Li, A.B.; Evgeniya Vaskova, Ph.D.; Connor O'Brien, M.D.; Ji Hye Jung, Ph.D.; Elizabeth Egan, M.D., Ph.D.; Jiangbin Ye, Ph.D.; Phillip Yang, M.D.

Online Methods:

Ethical approval

This study has been approved by Stanford University School of Medicine Institutional Review Board committee and Institutional Animal Care and Use Committee. (IRB Approval number: 31517, APLAC Approval number: 33723, and IACUC Assurance Number: A3213-01). All animals received humane care and treatment in accordance with the "Guide for the Care and Use of Laboratory Animals" (www.nap.edu/catalog/5140.html).

Preparation of human blood mononuclear cell-derived iPSCs and iCMs

The monoclonal iPSCs lines were generated by transfection of human blood mononuclear cells with non-integrating Sendai virus (Thermo Fisher Scientific, CA) as previously described (1, 2). iPSCs were maintained in Essential 8 medium (Thermo Fisher Scientific) and passaged every 4-days. iPSCs were chemically differentiated into iCMs as previously described (2). Briefly, 70-80% confluent iPSCs were incubated with differentiation medium, which consist of RPMI 1640 with serum free B-27 Supplement Minus Insulin (Thermo Fisher Scientific). On day 0-2, medium was supplemented with 6 μM CHIR-99021 (Selleck chemicals, TX), a glycogen synthase kinase 3β inhibitor. Then the medium was supplemented with C59 (Biolegend, CA), a Wnt inhibitor, on day 2-4. Upon spontaneous contractility (Days 9-10), medium was replaced to selection medium, which consists of RPMI 1640 without glucose with B-27 Supplement (Thermo Fisher Scientific) for the metabolic selection for 4-5 days. iCMs were replated on to new matrigel-coated 6-well plates and maintained with iCM culture medium (RPMI 1640 with serum free B-27 Supplement, Thermo Fisher Scientific). All medium, supplements and reagents we used in this study are extracellular vesicle (EV)-free and can be used for EV isolation (3).

Isolation of mitochondria-rich extracellular vesicles (M-EVs) and Large vesicle-depleted EVs (Ld-EVs)

iCM were plated onto 6-well plates (1,000,000 live cells/well) and cultured with RPMI 1640 with serum free B-27 Supplement for 48-hours. The conditioned-medium were collected and M-EVs were obtained based on a differential ultracentrifugation method. Floating cells, cell debris and apoptotic bodies were removed by centrifugation at 1,000g for 10-minutes at 4 °C. Pelleted vesicles were obtained by ultracentrifugation of the supernatant at 10,000g for 30-minutes at 4 °C. Ld-EVs were obtained by filtering of M-EVs through 220-nm polyvinylidene fluoride membrane filter. The counts and size distribution of EVs were determined by Nanoparticle tracking analysis (NTA) and flow cytometry (FCM) using size standard beads (Apogee Flow Systems, UK).

FCM-based EV analysis

Flow cytometry was conducted at the Stanford Shared FACS Facility (SSFF) on a BD LSRII instrument.

1. Preanalytical variables and experimental design

M-EVs or Ld-EVs were collected from iCMs conditioned-medium using the above-mentioned method. **Aim:** To compare mitochondria-positive rates or surface markers in M-EVs and Ld-EVs. **Keywords:** M-EV=mitochondria-rich extracellular vesicles, Ld-EVs=large vesicle-depleted extracellular vesicles, MTG=mitotracker green, MTDR=mitotracker deep red, WGA=wheat germ agglutinin. **Experimental variables:** M-EVs and Ld-EVs samples were collected from immature- or mature-iCMs.

2. Sample preparation

Sample preparation was performed as previously reported (4). $1x10^8$ EVs were washed and suspended in 200 μL of iCM culture medium and stained with 100 nM MTDR (Thermo Fisher Scientific, Waltham, MA), 100 nM MTG (Thermo Fisher Scientific), 1.25 μg/mL anti-human CD63 antibody (#12-0639-42, Thermo Fisher Scientific), 1.25 μg/mL anti-human β1-integrin antibody (Thermo Fisher Scientific), 1.25 μg/mL IgG1 kappa-PE isotype control (Thermo Fisher Scientific), 1.25 μg/mL IgG-APC isotype control (Thermo Fisher Scientific) or 1.0 μg/mL WGA Alexa Fluor 647 (Thermo Fisher Scientific) for 10-minutes at room temperature (RT) and protected from light. Antibody list can be found in Online Table 2.

3. Assay control

Buffer-only control of iCM culture medium, buffer with reagent controls, unstained controls and IgG isotype controls were measured at the same FCM settings as the EV-samples, including triggering threshold, voltages and flow rate. Unstained controls were used at the same dilution as stained and isotype controls. The event rate of buffer-only control was less than 1,500 events per second. Single-stained controls were used for validating compensation. We confirmed that iCM culture medium was EV-free (Online Fig. 12A). Less than 1% of EVs from mitochondria-free red blood cells (RBCs) were positive for mitochondrial markers (Online Fig. 12B). Neither serial sample dilution nor detergent treatment was performed.

4. Instrument calibration and data acquisition

Based on the buffer-only control and size-standard beads (Apogee Flow Systems), detection was triggered on the side scatter at a threshold of 215 arbitrary units. The flow rate was monitored using counting beads. Fluorescence calibration was performed using Rainbow Fluorescent Particles (Spherotech Inc, IL).

5. EV Characterization

EV diameter was approximated using the side scatter of the size standard beads (Online Fig. 12 C), as previously reported (5). We validated the approximation of EV size by filtration of the EV-samples with 220-nm filter (Online Fig. 12D).

6. FC data reporting

The concentrations of unstained EV-samples ranged from $1.0x10^9$ to $1.0x10^{10}$/mL. Flow cytometer acquisition settings were maintained for all samples including triggering threshold, voltages and flow rates. Data were analyzed using FlowJo (FlowJo, Ashland, OR).

Fluorescence-activated EV sorting

Vesicle sorting was performed as previously described (6-7). D15 M-EVs were stained with 100 nM MTG for 10-minutes at RT in PBS. M-EVs were washed and suspended in 500 μL PBS. MTG-positive EVs were sorted on a BD FACS Aria II using a 70 μm nozzle (Online Fig. 6A). Buffer-only control, size standard beads and unstained samples were used for control.

Nanoparticle tracking analysis (NTA)

Size and quantity of EVs were evaluated by NTA with a NanoSight LM20 (NanoSight, UK). EV-samples were washed with PBS and suspended in 1 mL PBS. Samples were loaded into the sample chamber with sterile syringes and imaged using a 40 mW at 640 nm laser. Three measurements of the same sample were performed.

***In vitro* hypoxia model**

iCMs that have been cultured for more than 40 days were used for hypoxia-injury models of cardiomyocytes. iCMs were placed in a Hypoxia Inductor Chamber (Stemcell Technologies, Canada). Oxygen content was reduced to 0.8-1.0% using N_2/CO_2 gas mix, and monitored continuously. The chamber was placed in a 37°C incubator for 24-hours.

Electron microscopy analysis

D15 M-EVs pellets were fixed in Karnovsky's fixative (2% glutaraldehyde, 4% paraformaldehyde, in 0.1 M sodium cacodylate pH 7.4) for 1-hour at RT. The fixative was replaced with cold/aqueous 1% osmium tetroxide and were then allowed to warm to RT for 2-hours rotating in a hood, washed 3 times with ultrafiltered water, then en bloc stained in 1% uranyl acetate at RT for 2-hours while rotating. Samples were then dehydrated in a series of ethanol (EtOH) washes for 30-minutes each at RT beginning at 50% followed by 70% EtOH then moved to 4 °C overnight. They were placed in cold 95% EtOH and allowed to warm to RT, changed to 100% EtOH 2 times, then followed by propylene oxide (PO) for 15-minutes. Samples were infiltrated with EMbed-812 resin (Thermo

Fisher Scientific) mixed 1:2, 1:1, and 2:1 with PO for 2-hours each left in samples of 2:1 ratio of resin to PO overnight, rotating at RT in the hood. The samples were then placed into EMbed-812 for 2 to 4-hours then placed into molds and fresh resin, oriented and placed into 65 °C oven overnight. Images were acquired with a JEM1400 120kV Transmission Electron Microscope with a Gatan Orius CCD Camera (JEOL, MA).

Isolation of mitochondria from iCMs

The Mitochondrial Isolation Kit for Cultured Cells (Thermo Fisher Scientific) was used for isolation of mitochondria from homogenized D15 (Isolated-Mito). Isolated mitochondria underwent FCM as previously described (8, 9). Isolated -mitochondria (1.0 μg/mL protein) in 500 μL of RPMI 1640 were stained with 100 nM MTDR for 10-minutes at RT and analyzed by BD LSR II.

Flow Cytometry (FCM)-based mitochondrial membrane potential and cell death assay.

Flow cytometry was conducted at the Stanford Shared FACS Facility (SSFF) on a BD LSRII instrument. Mitochondrial membrane potentials of iPSCs and iCMs were measured as previously described (10). iPSCs and iCMs were treated with 100 nM mitotracker deep red (MTDR, Thermo Fisher Scientific, Waltham, MA) and 100 nM mitotracker green (MTG, Thermo Fisher Scientific) at 37 ºC for 10-minutes. For the cell death assay, hypoxia-injured iCMs were treated with $3.0x10^8$/mL D15 M-EVs or Isolated-Mito at 3.0 μg/mL protein. Dead Cell Apoptosis Kit (Thermo Fisher Scientific) was used according to the manufacturer's instruction. Cells were washed with PBS and detached from dishes with TrypLE reagent and resuspended in cold PBS solution containing 1% Fetal Bovine Serum for FCM analysis.

3-(4,5-dimethylthiazol-2-yl)-2,5-diphenyltetrazolium bromide (MTT) assay

The MTT assays were performed according to the supplier's protocol (Sigma-Aldrich, MO).

Adenosine Triphosphate (ATP) measurement.

Intracellular and extracellular ATP was determined by CellTiter-Glo luminescence kit (Promega, G7570), which generates a luminescent signal proportional to the amount of ATP present. Opaque-walled 96-well plates with iCMs (10,000 cells/well) were prepared. CellTiter-Glo luminescence test solution was added and incubated for 30-minutes at RT. For the measurement of extracellular ATP (4), iCM culture medium (100 μL) containing M-EVs ($1.0 x10^8$) or Ld-EVs ($1.0 x 10^8$) were prepared. CellTiter-Glo luminescence test solution (100 μL) was added and incubated for 30-minutes at RT. Tissue ATP levels were measured according to manufacturer's protocol. Frozen heart tissues were homogenized in CellTiter-Glo Buffer and centrifuged at 14,000 rpm for 10-minutes.

Supernatants (50 μL) were mixed with 100 μL PBS. 2x CellTiter-Glo luminescence test solution (50 μL) was added and incubated for 10-minutes at RT. Luminescent signal was determined by a luminescence microplate reader.

Confocal microscopic analysis of mitochondria transfers *in vitro*.

Mitochondria were labeled with red fluorescent protein (RFP) or green fluorescent protein (GFP) using CellLight Mitochondria, BacMam2.0 according to the manufacturer's protocol (Thermo Fisher Scientific). BacMam is targeted to the mitochondrial matrix pyruvate dehydrogenase enzyme complex, ensuring fluorescence labeling of iCM-mitochondria. CellLight Mitochondria-RFP reagents (50 particles/cell) were added to D15 and incubated at 37°C for 24-hours. Cells were washed 2 times and cultured for 48-hours. The conditioned-medium were collected and M-EVs that contain RFP^+-mitochondria were obtained. RFP^+-Isolated-Mito were obtained from homogenized D15 that harbor RFP^+-mitochondria. iCMs transfected with BacMam mitochondria-GFP were subjected to hypoxia and treated with $3.0x10^8$/mL RFP^+-M-EVs (3.0×10^8/mL) or RFP^+-Isolated-Mito (3.0 μg/mL protein) for 3- or 24-hours. Cells were then rinsed twice and stained with Hoechst 33342. Images were acquired using an LSM 880 inverted confocal microscope (Zeiss, Germany).

Isolation of M-EVs collected from oligomycin A-treated D15 (Oligo-EV)

D15 were treated with 50 μM oligomycin A (Cayman Chemical) for 3-hours. iCMs were rinsed twice and medium was changed. Conditioned-medium was collected after 24-hour incubation and M-EVs (Oligo-EVs) were isolated by differential ultracentrifugation.

Real-time reverse transcription PCR (RT-PCR) test

Total RNA was purified from myocardial tissues or cells using TRIzol (Life Technologies) and miRNeasy Mini Kit (QIAGEN, Germany) according to the manufacturer's instructions. Total RNA from EVs was isolated using Total Exosome RNA Protein Isolation Kit (Thermo Fisher Scientific). RNA was reverse transcribed using High-Capacity RNA-to-cDNA Kit (Thermo Fisher Scientific). Equal amounts of cDNA were loaded onto a 96-well plate for RT-PCR using in-house primers and Power SYBR Green PCR Master Mix (Thermo Fisher Scientific). Relative gene expression was measured by Applied Biosystems™ StepOnePlus™ Real-Time PCR System (Thermo Fisher Scientific). Primers used are listed in Online Table 1.

Seahorse mitochondrial stress test

Oxygen consumption rate (OCR) of iCMs were measured using the Seahorse XF Extracellular Flux Analyzer (Agilent Technologies, CA). iCMs were plated at $1x10^4$ cells per well into the Seahorse

XF96 plate. Medium was replaced and pre-equilibrated for 40-minutes at 37℃. Mitochondrial stress test was performed following the direction in the XF Cell Mito Stress Test Kit (Agilent Technologies). After baseline OCR measurements, oligomycin A at 2.5 μM, carbonyl cyanide p-trifluoromethoxyphenylhydrazone (FCCP) at 5 μM and rotenone/antimycin A at 0.5/0.5 μM were sequentially injected to each well.

Mitochondrial DNA quantification

iPSCs and iCMs were collected and DNA was isolated using QIAamp Blood Mini Kit (QIAGEN). Quantification was performed by qPCR with SYBR green-based detection (Thermo Fisher Scientific). Relative mtDNA:nDNA ratio was calculated using the ΔΔCt method upon targeting nuclear-encoded genes (human *B2M* or mouse *GAPDH*) and mitochondrial-encoded genes (human *MT-TL1* or mouse *CYTB*). Primers used are listed in Online Table 1.

Western Blot Analysis

Each sample was loaded onto 4–20% Tris-glycine gels (Thermo Fisher). After electrophoresis and transfer to nitrocellulose membranes, the membranes were blocked in Tris-buffered saline containing 0.1% Tween 20 and 0.2% I-block (Tropix, T2015) for 60-minutes at RT. Membranes were then washed and incubated overnight at 4 °C with the primary antibodies. After incubation with peroxidase-conjugated secondary antibodies, visualization was enhanced by chemiluminescence. Optical density was assessed using the ImageJ software. Antibodies can be found in Online Table 2.

shRNA

D15 were plated in 6-well plates (300,000 live cells/well). Cells were treated with MISSION lentiviral transduction particles (Sigma-Aldrich) encapsulating non-targeting negative control shRNA (SHC016, sequence: CCGGGCGCGATAGCGCTAATAATTTCTCGAGAAATTATTAGCGCTATCGCGCTTTTT) or anti-PGC-1α shRNA (TRCN0000364085, sequence: CCGGTATGACAGCTACGAGGAATATCTCGAGATATTCCTCGTAGCTGTCATATTTTTG) at a MOI of 5. After 24-hours of transduction, cells were treated with puromycin at 3 μg/mL for 2-days to select transduced cells. Cells were incubated in culture medium for 48-hours and conditioned-medium was obtained to collect M-EVs.

Contractility analysis

iCM contractility was evaluated as previously described (11). iCMs were plated in 96-well plates (80,000 live cells/well) and exposed to 24-hours of hypoxia (0.8-1%) followed by 24-hours of

reoxygenation. 3.0x10^8/mL M-EVs or Isolated-Mito (3.0 μg/mL protein) were added at the time of reoxygenation. Cell membranes were stained with wheat-germ-agglutinin (Life Technologies, 17W11261) in FluoroBrite DMEM Media (Thermo Fisher) for 15 minutes at 37°C. Cells were washed and incubated in FluoroBrite DMEM for 15 minutes prior to imaging. Kinetic Image Cytometer 200 (Vala Sciences, San Diego, CA) at 100 Hz recorded a 6.5-second time series of iCMs using the automated microscopy platform.

Mitochondrial membrane potential assays of M-EVs and Isolated-Mito

Mitochondrial injury was induced by either Ca^{2+} ($CaCl_2$) or hydrogen peroxide (H_2O_2). PBS or mitochondria assay buffer (120 mM KCl, 10 mM Tris pH 7.6 and 5 mM KH_2PO_4) was used for the analysis of M-EVs or Isolated-Mito, respectively. Different concentrations of Ca^{2+} (0, 0.002, 0.02, 0.2 and 2 mM) or H_2O_2 (0, 1, 10, 100 and 1,000 mM) were prepared and 1.0 x 10^8/mL M-EVs or Isolated-Mito (1.0 μg/mL protein) were incubated for 3- or 24-hours. M-EVs and Isolated-Mito were then labeled with 100 nM MTDR for 10-minutes at 37 ºC and analyzed by FCM. 40 μM Carbonyl cyanide-4-(trifluoromethoxy)-phenylhydrazone (FCCP, Cayman Chemical) were used for control.

Mouse myocardial infarction (MI) model

Adult female CD1 mice (Age: 80-100 days) were purchased from Charles River. Experimental groups were randomized across multiple cages, litters, and location of mouse cages in the husbandry room. The murine model for MI was based on previously described methods (12). Mice were endotracheally intubated. Anesthesia was maintained with inhalational 1.5-2.0 % isoflurane. A thoracotomy was performed, and an 8-0 silk ligature was placed around the left anterior descending artery 1 mm below the atrioventricular border. It is reported that intramyocardial injection of EVs at 1.0 to 10 ug/g (EV-protein amount/mice body weight) improved post-MI cardiac function (13-15). In our pilot study, we determined that M-EVs at 9.58 ug/g was equalized to approximately 1x10^8 particles and subsequently used this dose. Mice were randomized into 6-groups and a blinded surgeon injected D15 M-EVs, D15 Ld-EVs, D50 M-EVs, D50 Ld-EVs (1 x 10^8/30 μL PBS/group), Isolated-Mitochondria (1.0 μg protein/30 μL PBS) or 30 μL PBS at 3-sites around infarct regions. The chest was closed, and animals were weaned from the ventilator and extubated.

Magnetic Resonance Imaging (MRI)

Cardiac MRI (Sigma 3T HDx, GE Healthcare, WI) was performed using a dedicated mouse coil (Rapid MR International, OH). Mice were imaged at week-2 and -4 after MI. Under anesthesia with 1-2% isoflurane, mice were placed in the supine position. Electrocardiographic gating was obtained with two subcutaneous precordial leads and body temperature was monitored with a rectal probe

during the entire scan (SA Instruments, NY). Left ventricular (LV) function was evaluated with EKG triggered Fast Spoiled Gradient-Recalled (FSPGR) sequence (TR 24ms, TE 10 ms, FA 45, field of view (FOV) 6 cm^2, matrix 256 Å~ 256, slice gap 0 mm, slice thickness 1 mm, NEX 4, 2 excitations, and 20 cardiac phases). Manganese-enhanced MRI (MEMRI) was performed using fast gradient echo-inversion recovery (FGRE-IR) sequence (TR 13 ms, TE 6 ms, FA 30°, FOV 4 cm2, matrix 256 Å~ 256, slice gap 0 mm, slice thickness 1 mm, 2R-R acquisition, TI 300-500 ms, and NEX 2) after 40 minutes with intraperitoneal injection of 0.7 cc/kg of SeeMore (Eagle Vision Pharmaceutical, PA) prior to MEMRI acquisition. The Mn^{2+}-based contrast agent in MEMRI is taken up by L-type calcium channel to generate T1-shortening and positive signal, conferring high specificity to the viable myocardium. The images were analyzed offline using Osirix (Pixmeo, Switzerland) with manual contouring. MEMRI tracing was generated for each short-axis slice and integrated to determine viable myocardial volumes in murine hearts. Percent MEMRI viable myocardial volume = MEMRI enhancement volume/total LV volume. All MRI data were analyzed by a blinded investigator.

Histological analysis of myocardial tissues

MTDR-labeled M-EVs (1.0×10^8/30 μL PBS) were injected into the peri-infarct region after induction of MI. Myocardial tissue samples were collected and embedded in the OCT compound at 8-hours after injection. 5 μm sections of the mid-ventricle were stained with cardiac troponin I (Thermo Fisher Scientific) and Hoechst 33342 according to the manufacturers' recommendations. Images were acquired using a LSM 880 inverted confocal microscope.

Statistical Analysis

Data are expressed as the mean ± standard deviations. We analyzed the differences between the two groups using unpaired *t*-tests; the differences among 3 groups or more were assessed using an ANOVA and post-hoc Tukey's or Bonferroni's multiple comparison tests with Prism Software version 4.0 (Graph Pad Software, CA). *P* values<0.05 were considered statistically significant. No adjustments of *P* values for multiplicity was performed, and therefore inferences drawn from these statistics may not be reproducible.

Online Tables:

Online Table 1. Primer List

Species	**Gene**	**Forward Sequence** (5'-3')	**Reverse Sequence** (5'-3')
Homo Sapiens	*ATP5A1*	AAGACACGCCCAGTTTCTTC	TTTGGGTTCATCTTTCATTGC
	ACTB	TCCCTGGAGAAGAGCTACGA	AGCACTGTGTTGGCGTACAG
	B2M	TGCTGTCTCCATGTTTGATGTATCT	TCTCTGCTCCCCACCTCTAAGT
	CAV3	GACCCCAAGAACATTAACGAGG	GGACAACAGACGGTAGCACC
	COX6A1	AGCCAGTTGGAAGTGGATTC	TGTACCTGAAGTCGCACCAC
	CS	GGGCTGCAAGAACAAGACA	CTCCCTTTCTTACCTCCCCA
	CYC1	GGTCACTGGCACTCACAGC	CCGCTACGGACACCTCAG
	ESRRG	GCTGTTCTCCGCATCTATCC	TGAAATCACAAAGCGCAGAC
	GJA5	AGAGTGTGAAGAAGCCCACG	AACAGATGCCAAAACTTCTGCT
	ITPR3	CCAAGCAGACTAAGCAGGACA	ACACTGCCATACTTCACGACA
	KCNH2	CAACCTGGGCGACCAGATAG	GGTGTTGGGAGAGACGTTGC
	MAPK1	TCTGGAGCAGTATTACGACCC	CTGGCTGGAATCTAGCAGTCT
	MYH7	TCGTGCCTGATGACAAACAGGAGT	ATACTCGGTCTCGGCAGTGACTTT
	NDUFA1	TTCTAGCAGGGGTAGATGGC	GAGATAGGCGCATCTCTGGA
	NPPB	TGGAAACGTCCGGGTTACAG	CTGATCCGGTCCATCTTCCT
	NRF1	CCACGTTACAGGGAGGTGAG	TGTAGCTCCCTGCTGCATCT
	PPARGC1a	AATTGAAGAGCGCCGTGT	AACCATAGCTGTCTCCATC
	PKM	TCACTATGGGGCTTCGACAT	ATAACCTTGAGGCTGAGGCA
	RYR2	CATCGAACACTCCTCTACGGA	GGACACGCTAACTAAGATGAGGT
	SDHA	CGAACGTCTTCAGGTGCTTT	AAGAACATCGGAACTGCGAC
	U6	CTCGCTTCGGCAGCACA	AACGCTTCACGAATTTGCGT
	TFAM	CCGAGGTGGTTTTCATCTGT	GCATCTGGGTTCTGAGCTTT
	MT-TL1	CACCCAAGAACAGGGTTTGT	TGGCCATGGGTATGTTGTTA

Species	Gene	Forward Sequence (5'-3')	Reverse Sequence (5'-3')
Mus Musculus	*ATP5I*	CCCCTGCTGAAATCCCTACA	TAAAACCACATCCACACCTC
	COX4I1	TTCAGTTGTACCGCATCCAG	GGATGGGGCCATACACATAG
	CYTB	CTTCATGTCGGACGAGGCTTA	TGTGGCTATGACTGCGAACA
	CYTC	AGAAGGGAGAAAGGGCAGAC	TGATCTGAATTTGGTGTGTGAA
	ESRRG	CAAGCGGACATCCTCGGG	GTAGCTAAGGTCCCTCGTGC
	GAPDH	AACTTTGGCATTGTGGAAGG	ACACATTGGGGGTAGGAACA
	NDUFAB1	CACCCCCACTGACGTTAGAC	TCGTCTTCCATGGCCATAAT
	NRF1	GCACCTTTGGAGAATGTGGT	CTGAGCCTGGGTCATTTTGT
	PPARGC1a	AAGTGTGGAACTCTCTGGAACTG	GGGTTATCTTGGTTGGCTTTATG
	SDHB	TGGTGGAACGGAGACAAGTA	TGGCAGCGGTAGACAGAGAA
	TFAM	AATTGCAGCCATGTGGAGGGA	GCTCTCAGGTGGGATGCAG

1

Online Table 2. Antibody Information

Antibody	Dilution	Manufacturer	Catalog No.
β-Actin	1:2,000	Millipore Sigma	A5441
COX IV	1:2,000	Cell Signaling Technology	11967
GAPDH	1:2,000	Santa Cruz Biotechnology	sc-25778
PGC-1α	1:1,000	Novus Biologicals	NBP1-04676
Troponin I	1:200	Thermo Fisher Scientific	701585
VDAC	1:1,000	Cell Signaling Technology	4661
Total OXPHOS	1:2,000	Abcam	Ab110411
Anti-Rabbit IgG	1:5,000	Promega	W4011
Anti-Mouse IgG	1:5,000	R&D	HAF007
CD29	1:1000	Thermo Fisher Scientific	17-0291-82
CD63	1:1000	Thermo Fisher Scientific	12-0639-42

Online Table 3. MRI parameters in the different experimental groups of mice

	sham	PBS	D15 M-EVs	D15 Ld-EVs	Isolated -Mito	D50 M-EVs	D50 Ld-EVs
N (per group)	6	8	8	8	8	8	7
Week-2							
LVEF (%)	55.9±3.5	19.2±2.9	32.8±4.8	26.4±3.6	22.3±2.5	21.3±3.3	23.3±2.8
LVEDV (μL)	57.4±13.1	183.6±25.7	112.7±23.4	141.8±30.0	158.3±21.5	157.0±11.4	155.0±18.5
LVESV (μL)	25.1±4.8	148.5±23.4	76.4±20.2	104.8±25.0	123.0±17.7	123.8±14.3	119.1±16.8
LV mass (mg)	55.7±5.6	98.3±11.6	70.2±10.6	92.1±14.4	93.1±10.6	90.0±14.7	95.3±9.4
Viability (%)	100.0±0.0	54.2±3.6	73.0±7.2	65.5±8.3	58.8±3.6	55.4±5.9	56.0±4.5
Week-4							
LVEF (%)	54.4±5.4	18.9±1.5	31.7±5.1	25.5±4.1	19.7±1.9	19.8±2.9	22.4±3.6
LVEDV (μL)	58.2±5.7	211.0±33.2	122.4±26.7	160.3±40.3	183.9±25.5	176.9±21.8	163.6±23.0
LVESV (μL)	26.7±5.5	171.4±29.1	84.4±23.5	120.3±35.9	151.0±19.8	142.3±22.1	127.7±23.1
LV mass (mg)	58.2±5.5	109.4±12.7	83.1±8.9	97.3±16.2	101.0±11.7	101.1±10.2	110.1±14.6
Viability (%)	100.0±0.0	53.8±5.3	74.1±7.5	65.7±6.8	56.8±4.1	55.8±4.1	59.3±2.5

Results are expressed as the mean ± SD. LVEF=left ventricular ejection fraction, LVEDV=left ventricular end-diastolic volume, LVESV=left ventricular end-systolic volume.

Online Figures and Legends

Online Figure. 1

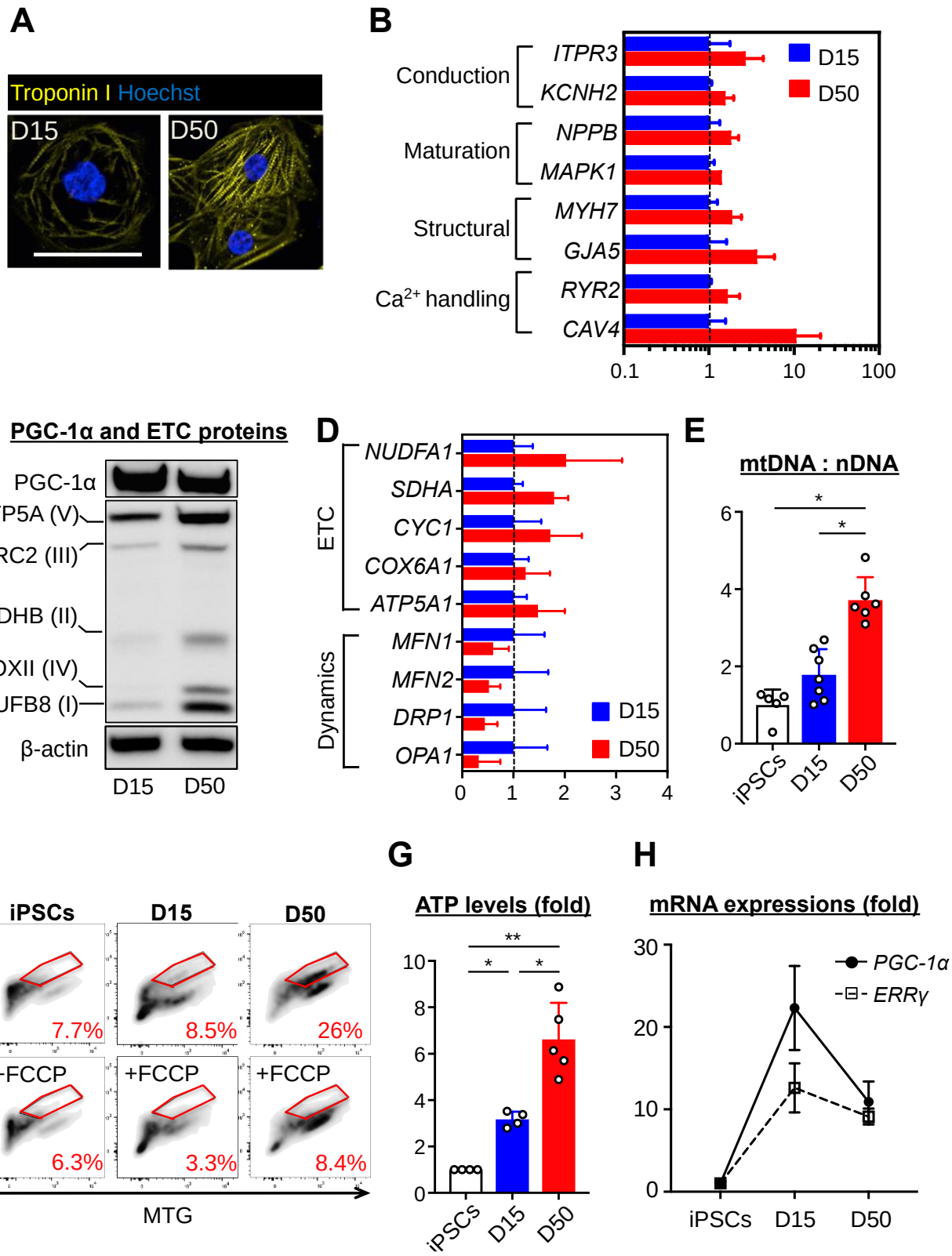

Online Figure 1. iCM mature in long-term culture (>50 days) through PGC-1α-mediated mitochondrial biogenesis. **A**. Representative images of D15 (early) and D50 (late). D50 demonstrated more organized sarcomere. Scale bar: 20 μm. **B**. Expression level of genes associated

with adult-like conduction (*ITPR3*, *KCNH2*), maturation (*NPPB, MAPK1*), ultrastructure (*MYH7, GJA1*) and calcium handling (*CAV3, RYR*), normalized to *ACTB* (n=4/group). **C.** Immunoblot analysis of D15 vs. D50. PGC-1α protein expression was upregulated in D15, whereas mitochondrial ETC proteins were upregulated in D50. **D**. The expression of genes associated with ETC complexes and mitochondrial dynamics, normalized to *ACTB* (n=4/group). **E.** Long-term culture increased relative mtDNA:nDNA ratio (n=5-7/group). **P*<0.0001 by a one-way ANOVA followed by Tukey's test. **F**. Representative FCM dot plots of D15 and D50. Cells were double stained with mitotracker deep red (MTDR) and mitotracker green (MTG). Long-term culture increased proportions of functional mitochondria. 2 mM carbonyl cyanide-4-(trifluoromethoxy)-phenylhydrazone (FCCP), which abrogates mitochondrial membrane potential, was used as a control. **G.** Intracellular ATP levels were increased in D50 (n=4-5/group). **P*<0.05 and **P<0.0001 by a one-way ANOVA followed by Tukey's test. **H**. *PGC-1α* and *ERRγ* mRNA levels, normalized to *ACTB*, were upregulated in D15 (n=5/group).

Online Figure. 2

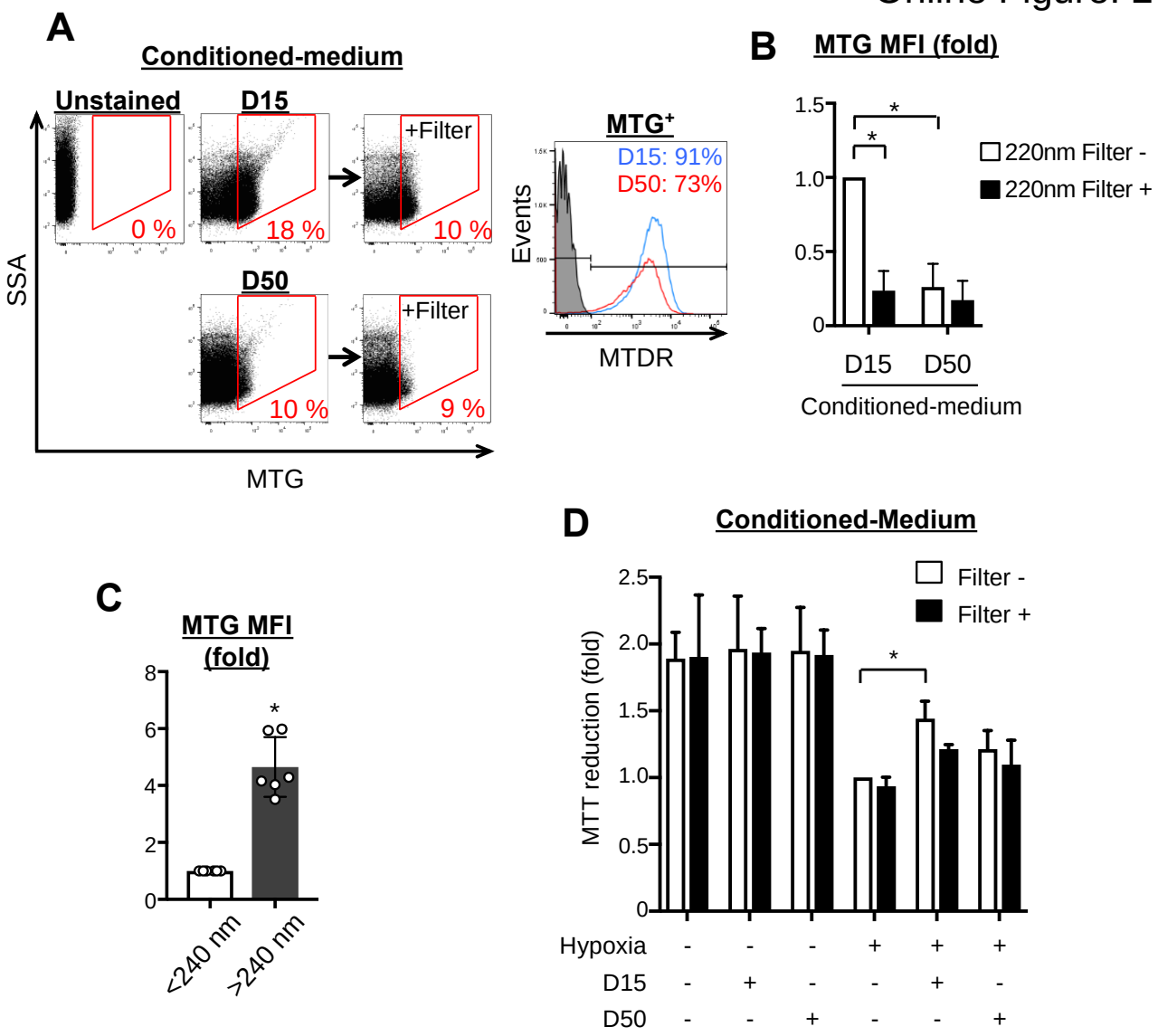

Online Figure 2. Extracellular mitochondria were predominantly incorporated by EVs with a diameter of larger than 220 nm. **A**. Representative FCM dot plots and histograms of conditioned-medium from D15 and D50. **B**. Quantitative analysis of MTG mean fluorescent intensity (MFI), an indicator of mitochondrial mass, was performed. D15 produced greater extracellular mitochondria than D50. 220-nm filter depleted a large fraction of extracellular mitochondria (n=4/group). **P*<0.0001 by a 2-way ANOVA followed by Bonferroni's test. **C**. Extracellular mitochondria were predominantly distributed in >240 nm range (n=6/group). **P*<0.0001 by an unpaired *t*-test. **D**. Conditioned-medium from D15, but not D50, increased 3-(4,5-dimethylthiazol-2-yl)-2,5-diphenyltetrazolium bromide (MTT) reduction as an indicator of mitochondrial function (n=5/group). **P*<0.05 by a 2-way ANOVA followed by Tukey's test.

Online Figure. 3

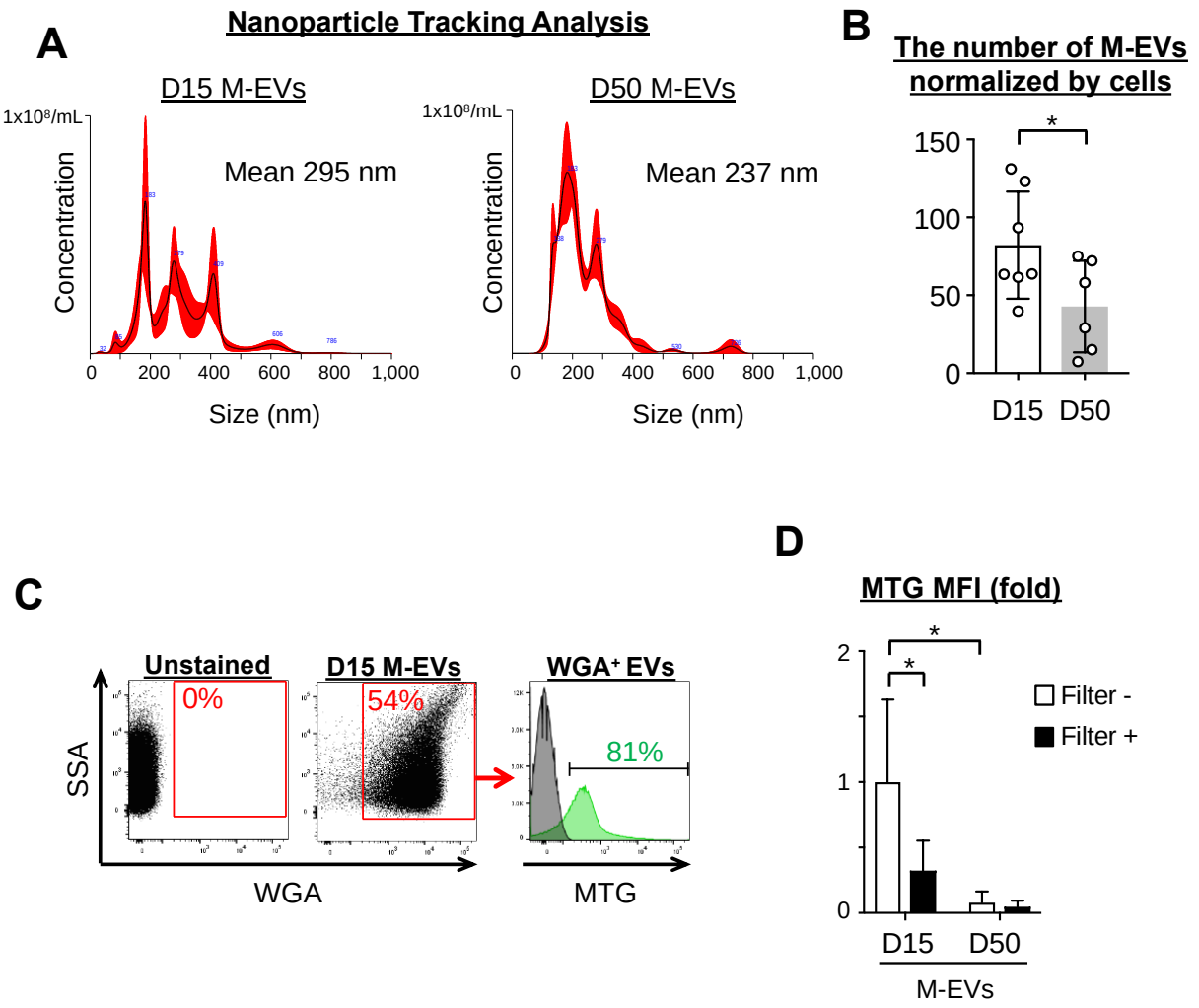

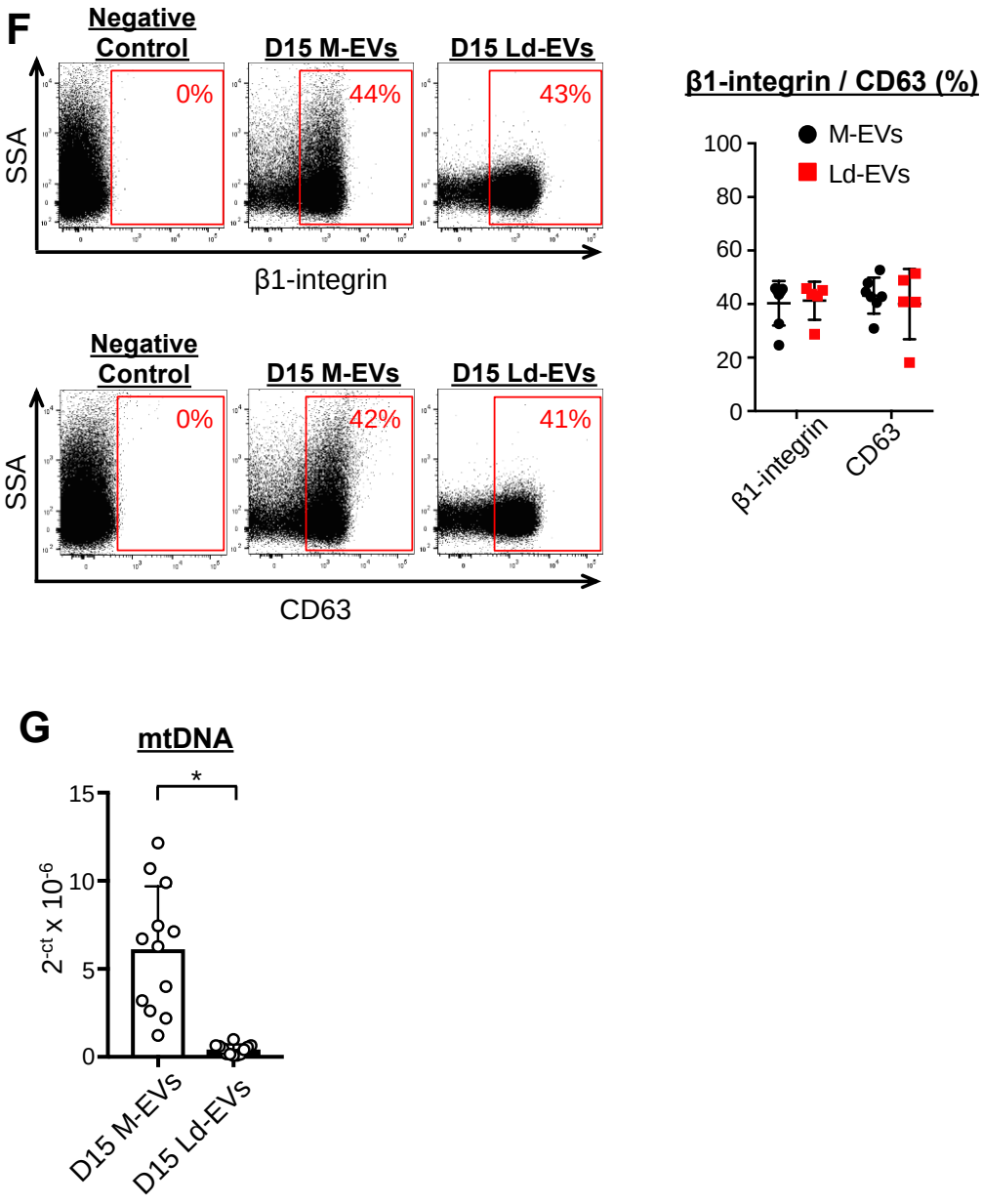

Online Figure 3. Characteristics of mitochondria-rich extracellular vesicles (M-EVs) and Large vesicle-depleted EVs (Ld-EVs.) **A**. Nanoparticles Tracking Analysis (NTA) of M-EVs from D15 and D50. **B**. The numbers of M-EVs from D15 vs D50. Data were normalized by cell count (n=6-7/group). *P<0.05 by an unpaired t-test. **C.** Representative FCM dotplots and histograms of D15 M-EVs stained with WGA and MTG. **D.** Quantitative analysis of MTG MFI. D15 M-EVs contained greater extracellular mitochondria than D50 M-EVs. 220-nm filter depleted a large fraction of extracellular mitochondria (n=6-10/group). *P<0.0001 by a 2-way ANOVA followed by Bonferroni's test. **E.** NTA of Ld-EVs from D15 and D50. **F.** FCM revealed that 40% and 43% of M-EVs were positive for β1-integrin and CD63, respectively (n=7/group). The positive rates for β1-integrin and CD63 in Ld-EVs were similar to those in M-EVs (41% and 40% respectively,

n=5/group). **G.** M-EVs, but not Ld-EVs, contained mitochondrial DNA (mtDNA, n=12/group). *P<0.0001 by an unpaired *t*-test. WGA=Wheat germ agglutinin; RBCs=red blood cells; MTDR=mitotracker deep red; MTG=mitotracker green; MFI=mean fluorescence intensity.

Online Figure. 4

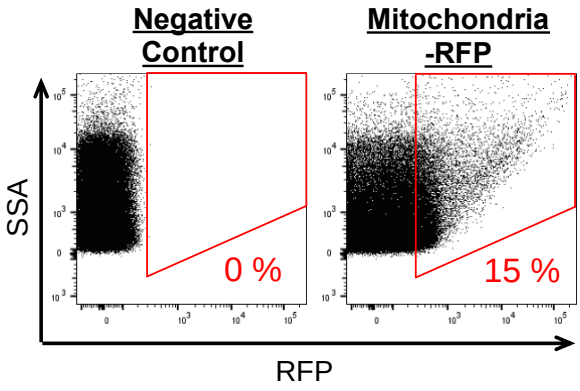

Online Figure 4. Representative FCM dot plots of M-EVs from D15 infected with BacMam CellLight Mitochondria-red fluorescent protein (RFP).

Online Figure. 5

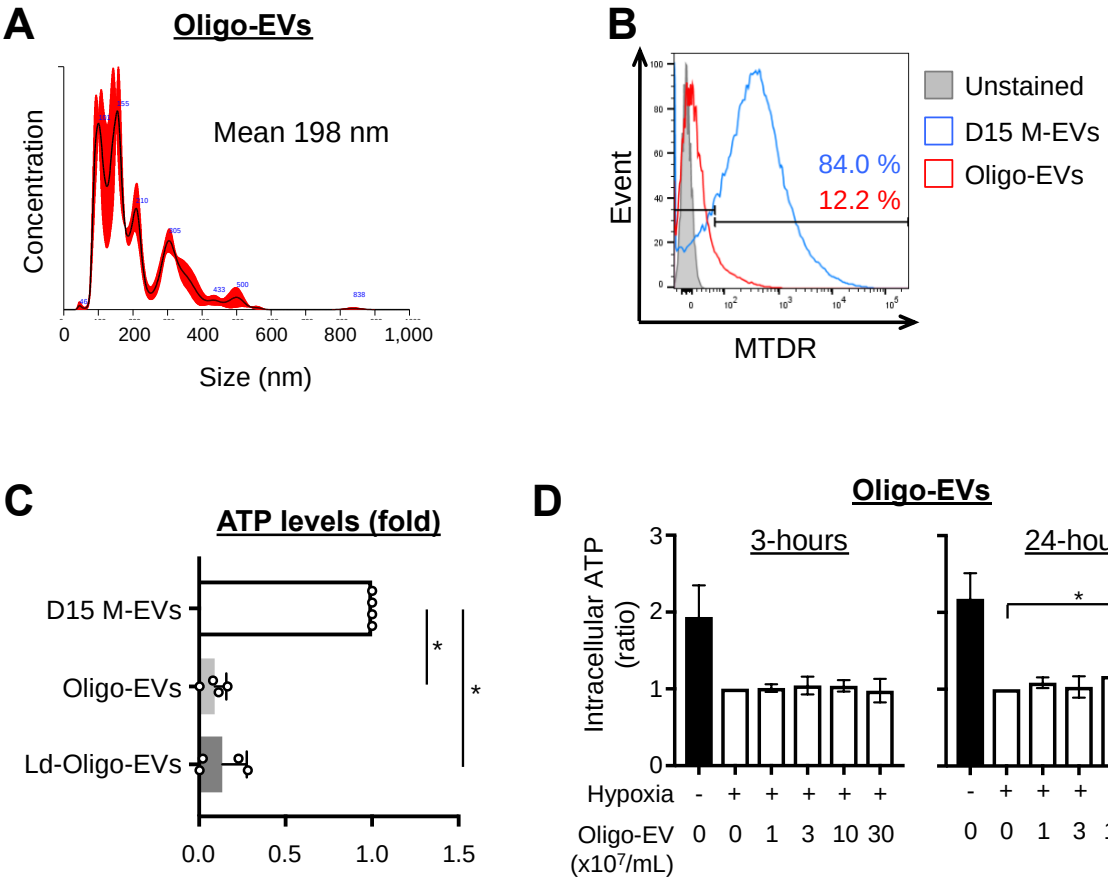

Online Figure 5. Characteristics of M-EVs from oligomycin A-treated D15 (Oligo-EVs). **A.** NTA of Oligo-EVs. **B.** FCM histogram of Oligo-EVs. FCM analysis with MTDR revealed that mitochondria inside the Oligo-EVs were dysfunctional. **C.** Oligo-EVs did not produce ATP (n=4/group). **P*<0.0001 by a one-way ANOVA followed by Tukey's test. **D.** Oligo-EVs restored ATP levels in hypoxia-injured iCMs. **Left**, 3-hours after treatment. **Right**, 24-hours after treatment (n=4/group). **P*<0.05 by a one-way ANOVA followed by Tukey's test.

Online Figure. 6

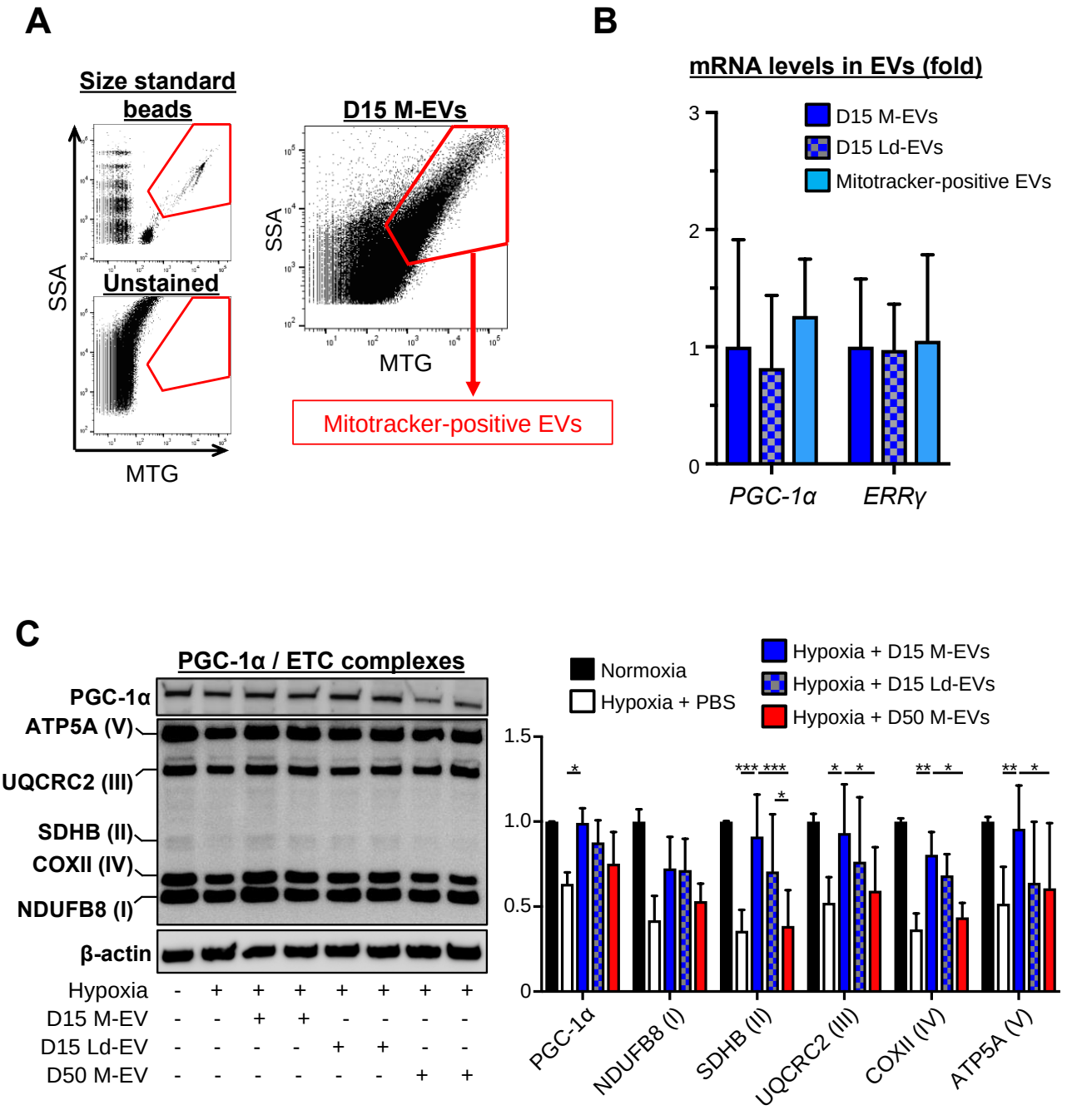

Online Figure 6. A. Gating strategy to sort Mitotracker-positive EVs. Size standard beads and unstained samples were used as control. **B.** *PGC-1α* and *ERRγ* mRNA levels, normalized to *U6*, in D15 M-EVs, D15 Ld-EVs and Mitotracker-positive EVs. No difference was observed (n=4-5/group). Data were analyzed by one-way ANOVA followed by Tukey's test. **C.** Representative immunoblots and quantitative analyses of PGC-1α, ETC complexes and β-actin (n=5-9/group). **P*<0.05, ***P*<0.01 and ****P*<0.001 by a one-way ANOVA followed by Tukey's test. Abbreviations as in Figure 1.

Online Figure. 7

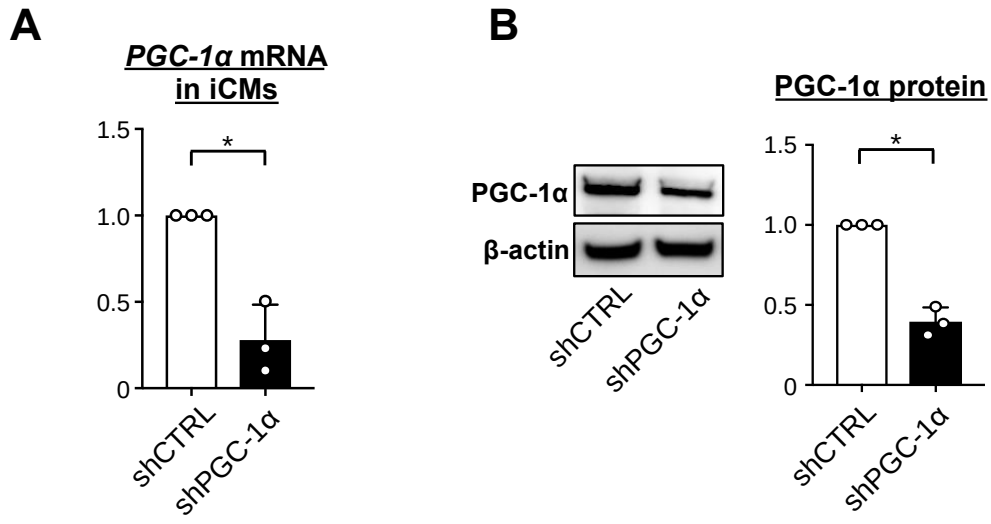

Online Figure 7. A. Relative *PGC-1α* mRNA expression, normalized to *ACTB*, in D15 transduced with *pLKO.1* expressing non-targeting shRNA (shCTRL) or anti-PGC-1α shRNA (shPGC-1α, n=3/group). **P*<0.01 by an unpaired *t*-test. **B**. Representative immunoblots and quantitative analyses of PGC-1α and β-actin in D15 transduced with shCTRL or shPGC-1α (n=3/group). **P*<0.0001 by an unpaired *t*-test.

v

Online Figure. 8

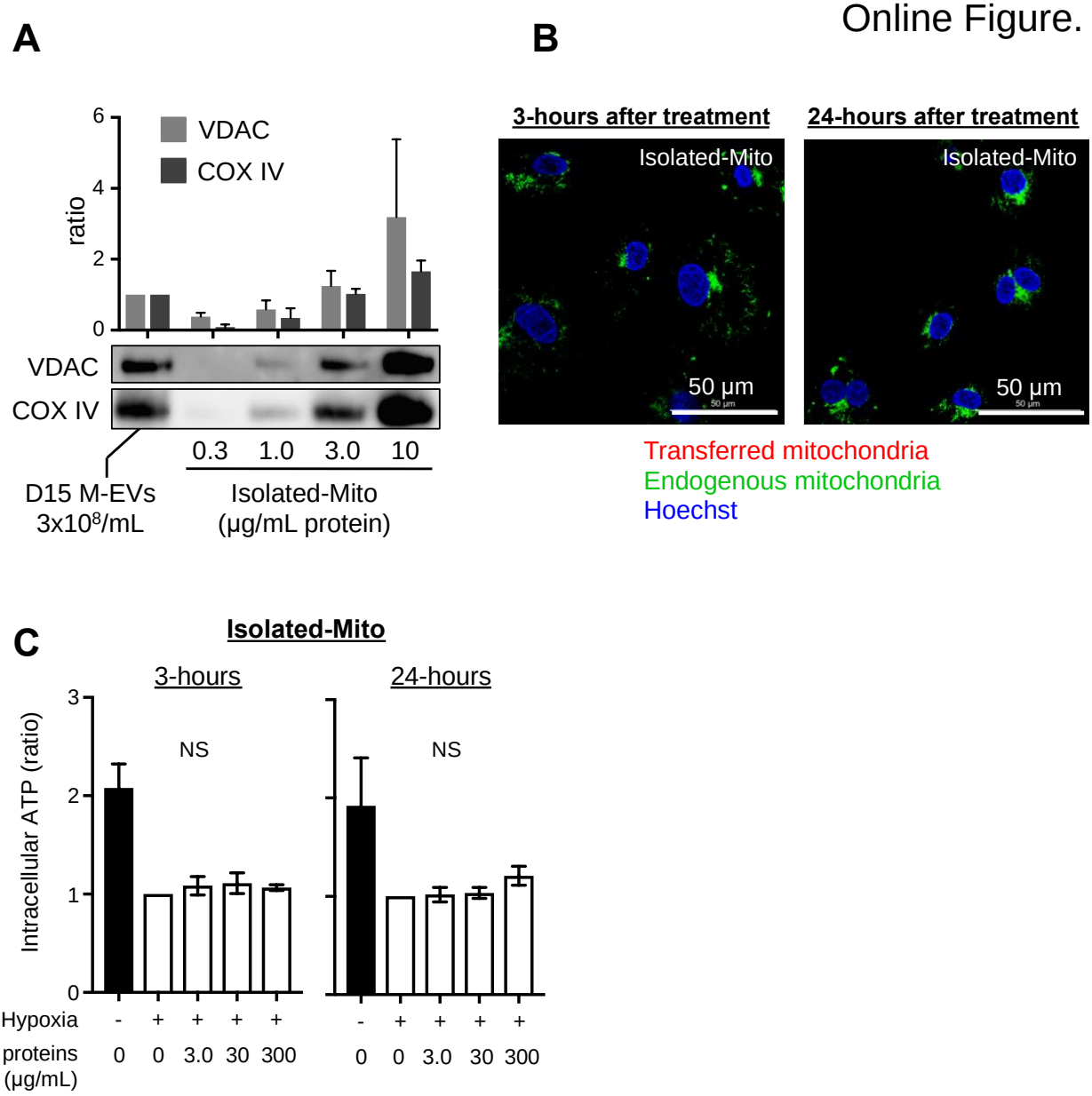

Online Figure 8. Isolated-mitochondria obtained from homogenized D15 (Isolated-Mito) did not restore mitochondrial bioenergetics in hypoxia-injured iCMs within 24-hours after treatments. **A.** Representative immunoblots and quantitative analysis of D15 M-EVs ($3.0x10^8$/mL) and Isolated-Mito (0.3-10 μg/mL protein) for voltage-dependent anion channels (VDAC) and cytochrome c oxidase subunit-4 (COX IV). Isolated-Mito (3.0 μg/mL protein) harbored the same amounts of mitochondrial proteins as $3.0x10^8$/mL M-EVs (n=2/group). **B.** Representative confocal microscopic image of iCMs treated with Isolated-Mito. Isolated-Mito (3.0 μg/mL protein) were obtained from D15 transfected with BacMam Mitochondria-RFP. iCMs transfected with BacMam Mitochondria-GFP were subjected to hypoxia for 24-hours and treated with RFP^+-Isolated-Mito for 3- or 24-hours.

Scale bar: 50 μm. **C**. Isolated-Mito did not increase ATP levels in hypoxia-injured iCMs. **Left**, 3-hours after treatment. **Right**, 24-hours after treatment (n=5/group). Data were analyzed by a one-way ANOVA followed by Tukey's test. NS=not statistically significant.

Online Figure. 9

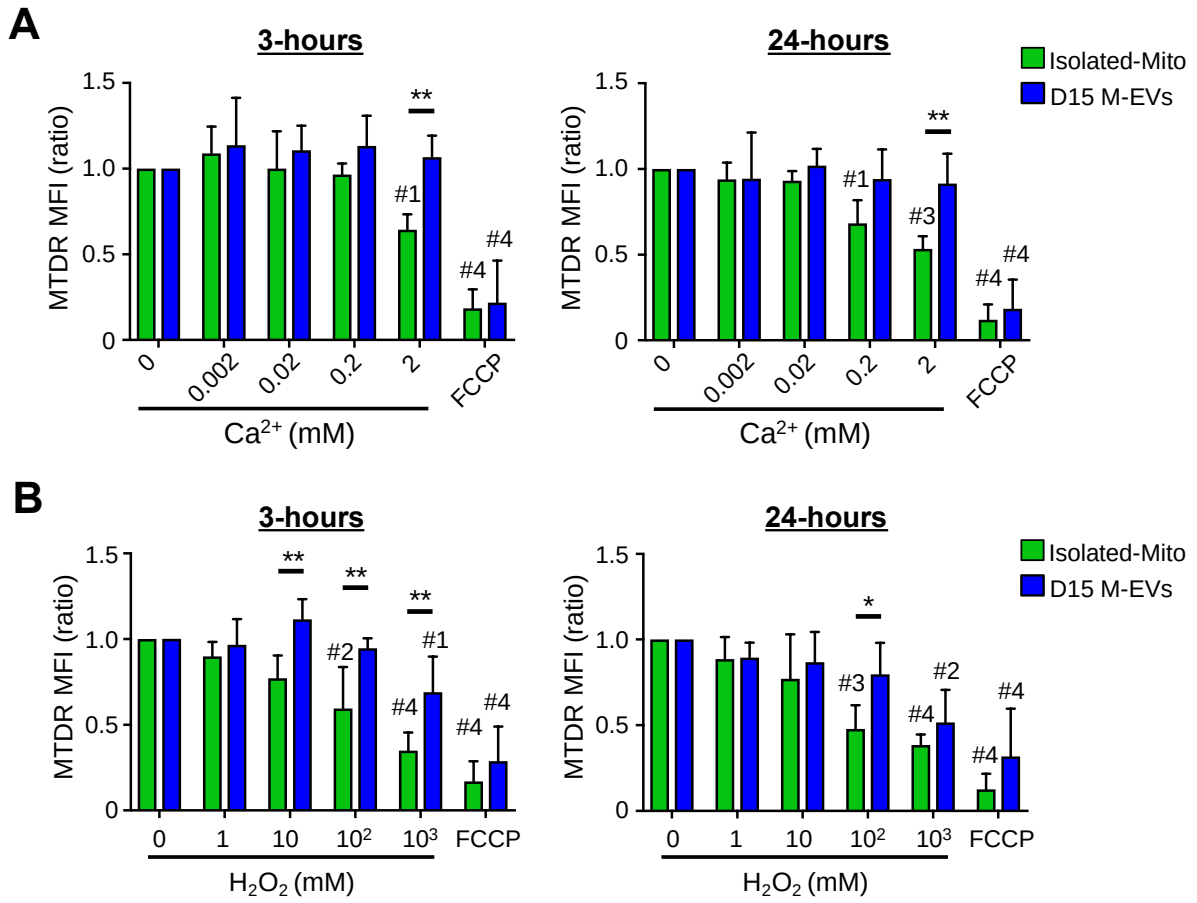

Online Figure 9. Mitochondria inside EVs are more resistant to Ca^{2+} overload and oxidative stress than isolated mitochondria. **A-B.** M-EVs or Isolated-Mito were incubated in different concentrations of Ca^{2+} (0.002-2 mM) or hydrogen peroxide (H_2O_2, 1-1000 mM) for 3- or 24-hours. Mitochondrial functions were evaluated by MTDR. 2 mM FCCP, which abrogates mitochondrial membrane potential, was used as a control (n= 4/group). **P*<0.05 and ***P*<0.01 by a 2-way ANOVA followed by Bonferroni's test. #1*P*<0.05, #2*P*<0.01, #3*P*<0.001 and #4*P*<0.0001 vs. control by a 2-way ANOVA followed by Tukey's test.

Online Figure. 10

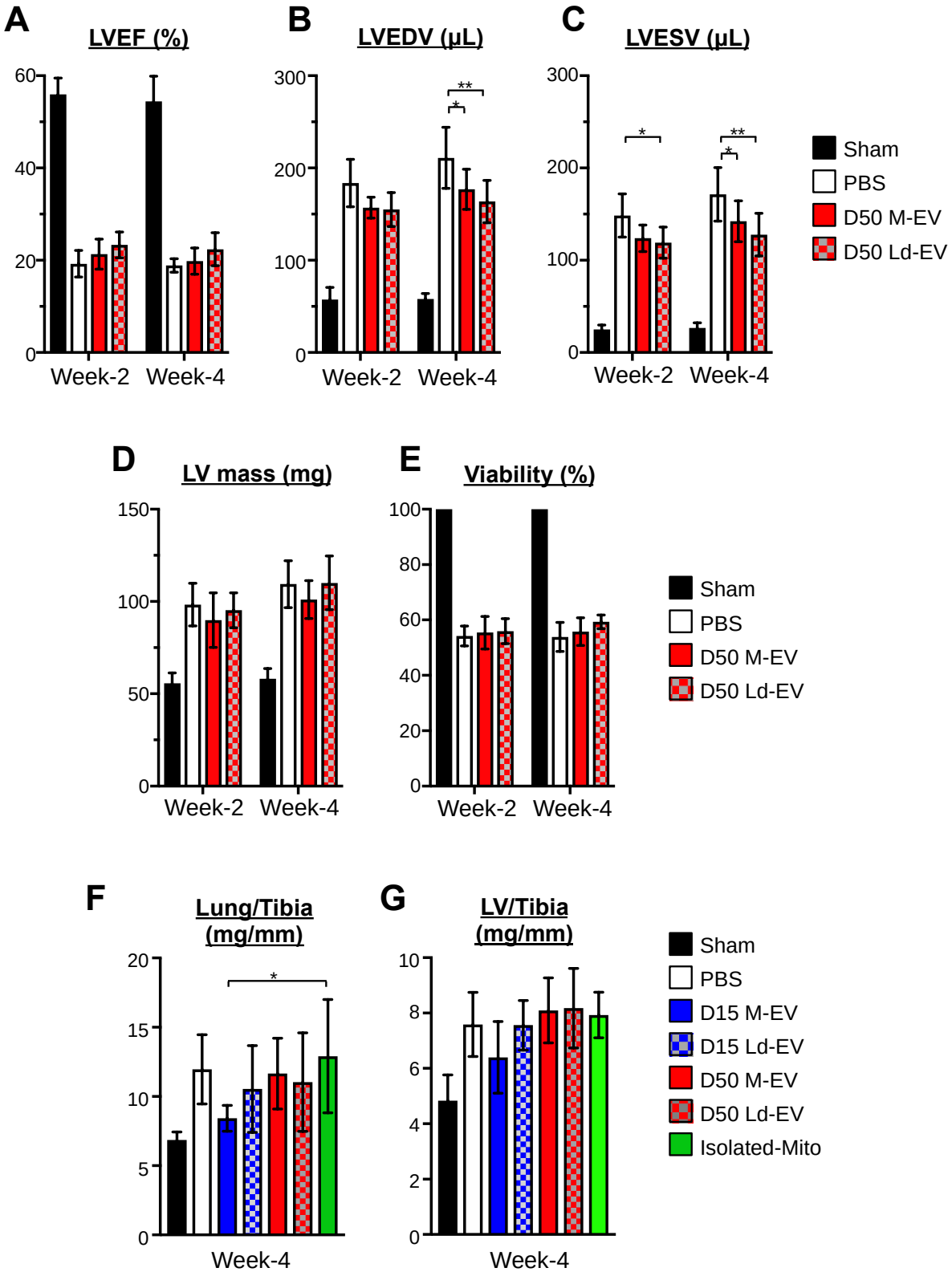

Online Figure 10. PBS (30 µL n=8), D50 M-EVs ($1x10^8$/30 µL PBS, n=8) or D50 Ld-EVs ($1x10^8$/30 µL PBS, n=7) were injected into the 3 sites of peri-infarct region. **A to E**. LV ejection fraction (LVEF), LV end-diastolic volume (LVEDV), LV end-systolic volume (LVESV), LV mass

and myocardial viability at week-2 and -4 after myocardial infarction (MI), evaluated by MRI. *P<0.05 and **P<0.01 by a 2-way ANOVA followed by Tukey's test. **F**. Lung weight to tibia length (TL) (lung/tibia) ratio. **G**. LV weight to TL (LV/tibia) ratio (n=7-8/group). *P<0.05 by a one-way ANOVA followed by Tukey's test.

Online Figure. 11

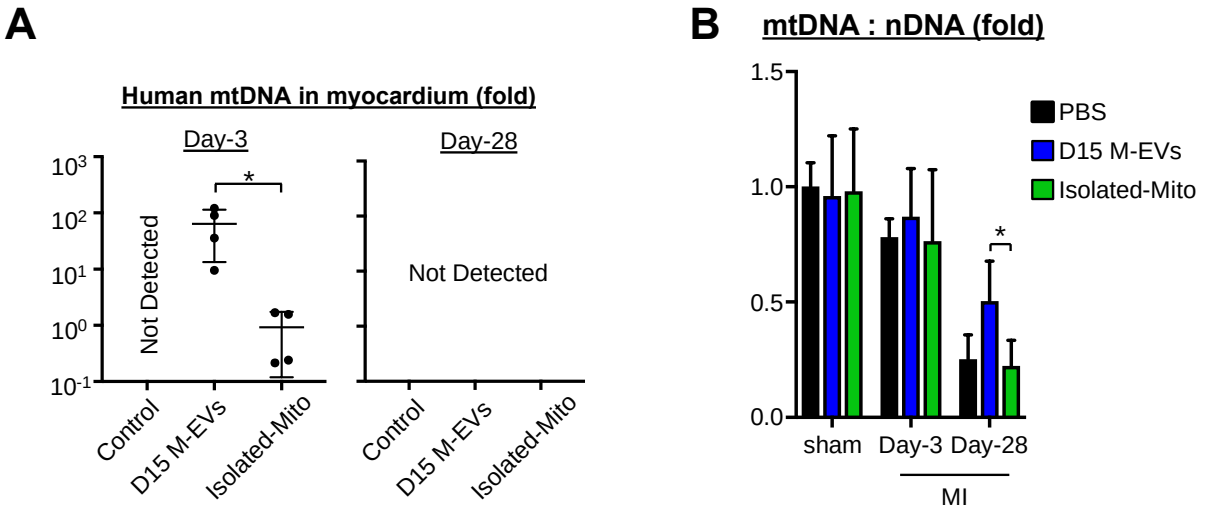

Online Figure 11. A. Human-derived mtDNA was detected in mice myocardium at day-3 as determined by PCR; shown as fold change relative to Isolated-Mito treated myocardium (n=4/group). **P*<0.05 by an unpaired *t*-test. **B.** mtDNA copy number were measured by PCR (n=4-6/group) **P*<0.05 by a 2-way ANOVA followed by Tukey's test.

Online Figure. 12

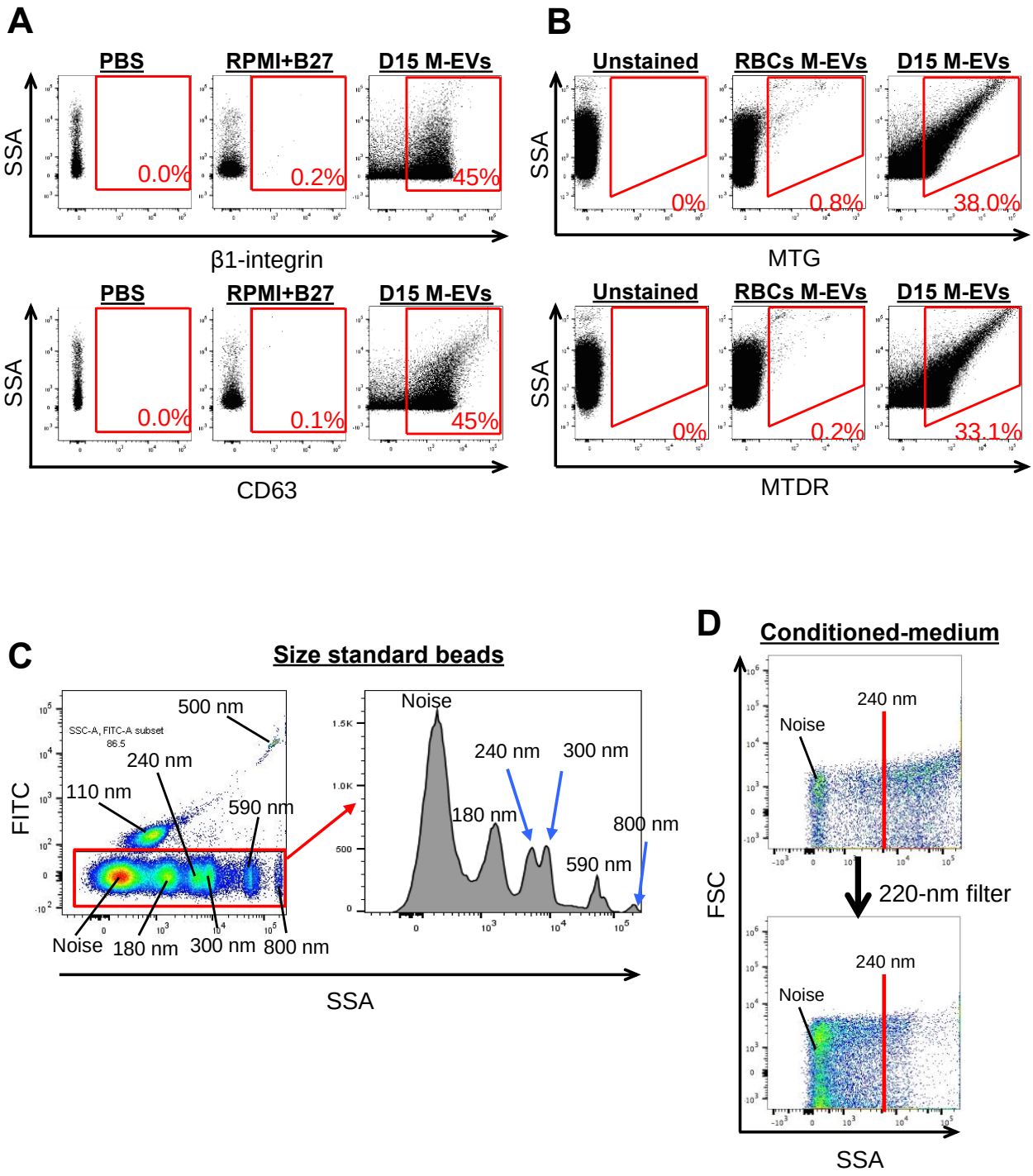

Online Figure 12. A. Representative FCM dotplots of PBS, iCM culture medium (RPMI 1640+B27) and D15 M-EVs. **B.** Representative FCM dotplots of EVs from RBCs and D15 M-EVs. **C**. Representative FCM dot plots and histogram of size-standard beads. The beads size below 1 μm range was separated by the side-scatter-area (SSA). **D**. FCM dot plots of conditioned-medium. Filtration with 220-nm filters depleted EVs with a diameter of larger than 240 nm measured by the SSA.

Reference

1. Ge X, Wang I-NE, Toma I, et al. Human Amniotic Mesenchymal Stem Cell-Derived Induced Pluripotent Stem Cells May Generate a Universal Source of Cardiac Cells. *Stem Cells Dev*. 2012;21:2798–2808.
2. Burridge PW, Matsa E, Shukla P, et al. Chemically defined generation of human cardiomyocytes. *Nat Methods*. 2014;11:855–860.
3. Ong SG, Lee WH, Zhou Y, et al. Mining Exosomal MicroRNAs from Human-Induced Pluripotent Stem Cells-Derived Cardiomyocytes for Cardiac Regeneration. *Methods Mol Biol*. 2018;1733:127-136.
4. Hayakawa K, Esposito E, Wang X, et al. Transfer of mitochondria from astrocytes to neurons after stroke. *Nature*. 2016;535:551–555.
5. Coronado M, Fajardo G, Nguyen K et al. Physiological Mitochondrial Fragmentation Is a Normal Cardiac Adaptation to Increased Energy Demand. *Circ Res*. 2018 Jan 19;122(2):282-295.
6. Higginbotham JN, Demory Beckler M, Gephart JD, Franklin JL, Bogatcheva G, Kremers GJ, Piston DW, Ayers GD, McConnell RE, Tyska MJ, Coffey RJ. Amphiregulin exosomes increase cancer cell invasion. Curr Biol. 2011 May 10;21(9):779-86.
7. McConnell RE, Higginbotham JN, Shifrin DA Jr, Tabb DL, Coffey RJ, Tyska MJ. The enterocyte microvillus is a vesicle-generating organelle. J Cell Biol. 2009 Jun 29;185(7):1285-98.
8. Medina JM, López-Mediavilla C, Orfao A. Flow cytometry of isolated mitochondria during development and under some pathological conditions. *FEBS Lett*. 2002;510:127–132.
9. Mattiasson G. Flow cytometric analysis of isolated liver mitochondria to detect changes relevant to cell death. *Cytometry A*. 2004;60:145–154.
10. Zhou R, Yazdi AS, Menu P, Tschopp J. A role for mitochondria in NLRP3 inflammasome activation. *Nature*. 2011;469:221–225.
11. Sharma A, Burridge PW, McKeithan WL, et al. High-throughput screening of tyrosine kinase inhibitor cardiotoxicity with human induced pluripotent stem cells. *Sci Transl Med*. 2017;9:eaaf2584.
12. Tachibana A, Santoso MR, Mahmoudi M, et al. Paracrine Effects of the Pluripotent Stem Cell-Derived Cardiac Myocytes Salvage the Injured Myocardium. *Circulation Research*. 2017;121:e22–e36.
13. Zhao J, Li X, Hu J, Chen F, Qiao S, Sun X, Gao L, Xie J, Xu B. Mesenchymal stromal cell-derived exosomes attenuate myocardial ischaemia-reperfusion injury through miR-182-

regulated macrophage polarization. Cardiovasc Res. 2019 Jun 1;115(7):1205-1216. doi: 10.1093/cvr/cvz040.

14. Adamiak M, Cheng G, Bobis-Wozowicz S, et al. Induced Pluripotent Stem Cell (iPSC)-Derived Extracellular Vesicles Are Safer and More Effective for Cardiac Repair than iPSCs. *Circ Res*. 2018;122(2);296-309.

15. Zhu LP, Tian T, Wang JY, et al. Hypoxia-elicited mesenchymal stem cell-derived exosomes facilitates cardiac repair through MiR-125b-mediated prevention of cell death in myocardial infarction. *Theranostics*. 2018;8:6163–6177.